

Analysis of the Cool Roof Effect through a Building Modeling Experiment

Gyeongah Kim¹, Kyunghun Park^{2*}, Bonggeun Song³, Dain Jeong⁴,
Chulhyun Choi⁵, Kyeongho Seo⁶



¹ Department of Environmental Engineering of Changwon National University, 20 Changwondaehak-ro Uichang-gu Changwon-si, Gyeongsangnam-do 641-773, Rep. of KOREA, wing1128@naver.com

² Department of Environmental Engineering of Changwon National University, 20 Changwondaehak-ro Uichang-gu Changwon-si, Gyeongsangnam-do 641-773, Rep. of KOREA, landpkh@changwon.ac.kr *Corresponding author

³ National Institute of Ecology, 1210 Geumgang-ro Maseo-myeon Seocheon-gun, Chungcheongbuk-do 325-813, Rep. of KOREA, bgsong@nie.re.kr

⁴ Department of Environmental Engineering of Changwon National University, 20 Changwondaehak-ro Uichang-gu Changwon-si, Gyeongsangnam-do 641-773, Rep. of KOREA, dohundain@naver.com

⁵ Dept. of Landscape Architecture of Kyungpook National University, 80 Daehak-ro Buk-gu, Daegu, Republic of Korea, 702-701, kenix@naver.com

⁶ Department of Environmental Engineering of Changwon National University, 20 Changwondaehak-ro Uichang-gu Changwon-si, Gyeongsangnam-do 641-773, Rep. of KOREA, seokh135@naver.com

1. Introduction

According to the United Nations (U.N.), 54% of the world's population lived in cities in 2014. Urban populations have increased by 34% since 1960, and this growth continues today [1]. The increase in urban population has naturally led to an increase in artificial land cover in cities [2]. Accordingly, land cover changes of cities have led to the creation of urban heat islands (UHI) [3, 4, 5].

To address the challenge of UHIs, measures such as cool roofs, green roofs, and wind corridors have been employed in cities around the world [6, 7]. In South Korea, green roofs have been widely used for the mitigation of UHIs, but they are difficult to install on existing buildings, which have deteriorated due to increased load stress. Because dilapidated buildings make up a large percentage of existing structures in cities, providing feasible UHI measures that can be applied to these buildings is important. Thus, recent investigations have focused on cool roofs, which may help to maintain the integrity of existing buildings while producing heat-mitigating effects.

In the current study, the cool-roof method was applied in South Korea, located in a mid-latitude temperate climate zone, and the results were evaluated. For objective comparison, small-scale building models were created and monitored for approximately one year.

2. Experimental Methods

2.1 Construction and installation

Because most roofs in South Korea are flat, small-scale building models were designed to be hexahedrons with respective lengths, widths, and heights of 1,000 mm. Taking the material and color of the roofs into consideration, nine building models were created. However, only five of the buildings are referenced in the present study; the other four were excluded because of partial data loss or because data gathered from them were inadequate for comparison of the relevant effects. Expanded polystyrene panels were used to insulate the models. The insulator's thermal conductivity was 0.035–0.040 W/m²K. Insulator thickness was selected in accordance with South Korea's Building Design Criteria for Energy Saving. When buildings were exposed to open air, thermal transmittance was below 0.220 W/m²K for the roof, below 0.340 W/m² K for the outer wall, and below 0.330 W/m²K for the floor; thus, in order to emulate these conditions as closely as possible, the thickness of the insulator was set to 150 mm for the roof, 100 mm for the outer wall, and 100 mm for the floor (Fig. 1). Finally, before the roofs were installed, the models were inspected to confirm that the dimensions were identical.

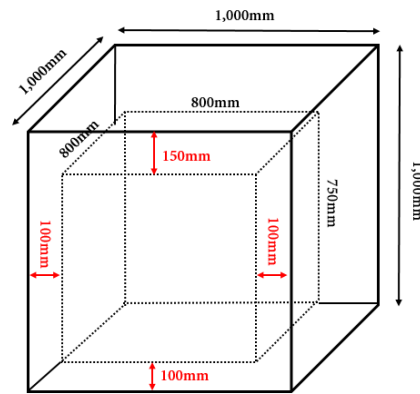


Fig 1. Blueprint for the small-scale building model.

2.2 Types of roof

All factors, excluding the roof, were identical across all models. The materials and colors most frequently used in Korea were considered when selecting the roofs to be used.

The most commonly used asphalt shingles and paint in South Korea were selected. Green, the most common roof color in South Korea was used. White and black were also selected to represent bright and dark colors. For comparison with the cool-roof method, green roofs were also used.

Table 1. Roof types and colors.

Model	Material	Color	Average reflectivity	Average emissivity
P-G (Paint, green)	Paint	Green	0.112	0.807
P-W (Paint, white)	Paint	White	0.596	0.886
P-B (Paint, black)	Paint	Black	0.043	0.811
A-W (Asphalt shingle-white)	Asphalt Shingle	White	0.555	0.875
GR (Green roof)	Green Roof	-	0.100	0.898

2.3. Description of the experimental site

A small-scale building model was installed in the city of Changwon, which is located in the southern region of South Korea. Although South Korea is located in a mid-latitude temperate climate zone and therefore does not experience constant hot temperatures, UHIs are developing because of the high density of South Korean cities. To ensure that the results were influenced by roof type only, the models were separated by a length of 2m and a width of 2m to eliminate shadows between the buildings. Furthermore, the models were installed on the rooftop of a school to guarantee that no shadows were cast upon them by tall buildings in the vicinity.

To ensure reliability of the results, the surface temperatures of the roof and indoor temperatures of the completed model were measured between April 18 and 29, 2014, prior to roofing the models. Afterward, the fully constructed models were measured for one year, from May 29, 2014, to May 30, 2015. Any inconsistencies in measurement attributed to either technological or natural phenomena were not included in the results. In the current study, data gathered in the summer months, June, July, and August, of 2014 were used.

3. Instrumentation and measured variables

3.1 The surface temperature of roofs and indoor temperatures

To obtain an accurate temperature measurement for the roof surface, a contact surface thermometer was used (Testo 175 T3; accuracy: ± 0.5 °C); measurement intervals were set to 1 min. To understand the characteristics of temperature distribution in graphic form, thermographic cameras (Testo 876) were used for measurement from 11 a.m. to 4 p.m. local time on May 30, 2014. To measure indoor temperatures, thermometers were installed 15 cm above the floors of the models (Testo 175 H1; accuracy: ± 0.4 °C), and the measurement intervals were set to 1 min.

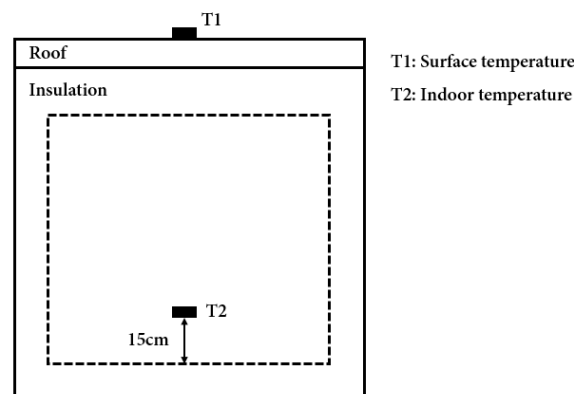


Fig 2. Temperature measurement points in the model.

3.2 Reflectivity, emissivity, and net radiant energy

To investigate the reflectivity, emissivity, and net radiant energy of the different roof types, measurements were made from 9 a.m. to 3 p.m. local time on July 31, 2014. A CNR4 Net Radiometer was used to measure roof reflectivity and terrestrial radiant energy. Because emissivity cannot be measured, the Stefan–Boltzmann formula was for calculation. The measured reflectivity and emissivity are displayed in Tables 1 and 3. The formula can be expressed as

$$\varepsilon_i = \frac{L_i}{\varepsilon_{0.95} \times \sigma \times (273.15 + T_{si})^4},$$

where ε_i represents the emissivity of the roof finishing materials; L_i , terrestrial radiant energy measured with the CNR4 net-radiometer on the roof's finishing materials; $\varepsilon_{0.95}$, the emissivity selected via the thermal thermometer (0.95); T_{si} the surface temperature of the roof measured using the thermal thermometer; and σ , the Stefan–Boltzmann constant ($5.67 \times 10^{-8} \text{ Wm}^{-2}\text{K}^{-4}$).

Results

1. Comparison of models

The roof surface temperature measured from April 18 to 21, 2014, was analyzed by using the root-mean-square error (RMSE). Of the five models, P-G (paint, green) was taken as the standard, and the RMSE for each of the remaining four models were calculated.

For roof surface temperatures, the maximum RMSE value was 1.15 °C, and the margin of error of the measuring equipment, particularly the contact surface thermometer, was ± 0.5 °C. Thus, the RMSE likely did not significantly affect the measured roof surface temperature values. The maximum RMSE value for indoor temperatures was 0.37 °C, and the margin of error of the measuring equipment, particularly the thermo-hygrometer, was ± 0.4 °C. Thus, the RMSE likely did not significantly influence indoor temperature values.

Table 2. Root-mean-square error (RMSE) analysis results.

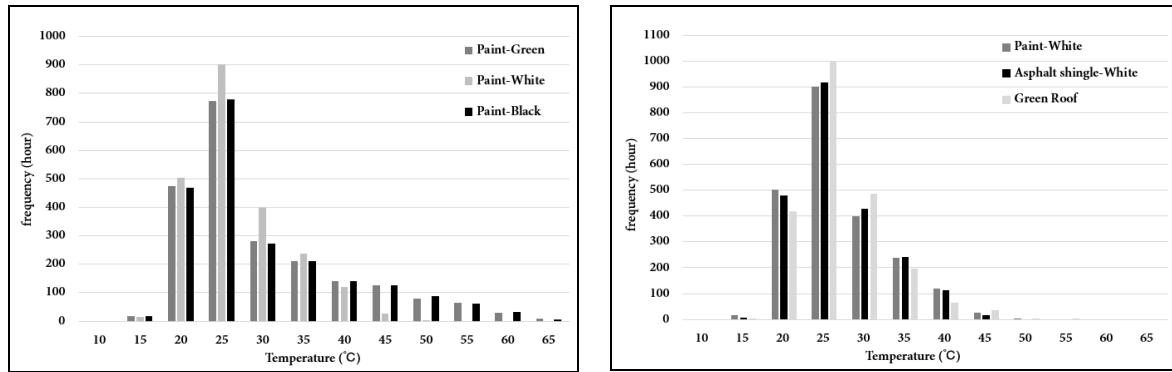
	P-W	P-B	A-W	GR
Roof temperature	0.73	0.65	1.15	0.54
Indoor temperature	0.13	0.37	0.24	0.33

2. Roof surface temperature

Roof surface temperatures are associated with the effects of UHIs. That is, when low surface temperatures are maintained, UHI effects may be mitigated. Figure 2 shows a histogram of roof surface temperatures according to roof type. The units used for the frequency are hours (h). For example, a frequency value of 1 for 10 °C indicates that a roof surface temperature of 10 °C was measured for 1 h.

Figure 3 shows the changes in roof surface temperature according to roof color. Paint was used as the coloring material for the roofs in all models. For white roofs, no measurements were in high temperature ranges of greater than 50 °C. However, green and black roofs showed high frequencies of measurement at high temperature ranges. The frequencies of measurement for green and black roofs were similar for all temperature ranges, which meant that roof surface temperatures for green roofs are just as high as those of black. Thus, given that most roofs in South Korea are green, surface temperatures during the summer are likely to be high and can cause UHI effects. Changes in roof surface temperature according to roof material are shown in Figure 4. The color for all roofs was fixed to white. Compared with color, temperature changes caused by differences in material were small. For a detailed comparison, the average temperature during a 24 h period in summer 2014, 24 °C, was set as the standard. The frequencies of temperatures rising above this standard were combined for comparison. At 1,688 h

and 1,722 h for paint and asphalt shingles, respectively, asphalt shingles had higher frequencies of temperature measurements in high-temperature ranges.



Surface temperature according to roof color.

Surface temperature according to roof material.

Fig 3. Changes in roof surface temperature according to roof type.

The measurements made with thermographic cameras are displayed in Table 3. M1 and M2 marked on each roof surface indicate areas for temperature measurement; the temperature ranged from a low of 30 °C to a high of 52.5 °C. The temperatures at M1 and M2 on the same roof may have differed while using the thermographic camera because of the difference in the angle or distance between the camera and the roof. In addition, various emissivity values must be selected according to roof material; however, because the same emissivity was selected for all roofs, it was difficult to observe actual roof surface temperature. Because infrared light can be visualized, however, roof surface temperatures may be effectively compared on a relative level.

The results show that brighter roof color relates to lower surface temperatures and that the difference in temperatures according to roof materials was not large. In the case of green roofs, the temperature of the vegetation was lower than that of the soil. Thus, if green roofs are to be used as a measure for the mitigation of UHI effects, a sufficient amount of vegetation should be planted. The surface temperatures of green roofs measured by using the contact surface thermometer refer to the soil temperature.

Table 3. Types of roof finishing materials.

Material	Paint	Paint	Paint
Color	Green	White	Black
Image			
Surface temperature	M1: 45.8 °C, M2:47.4 °C	M1: 31.8 °C , M2: 31.6 °C	M1: 47.7 °C , M2: 47.3 °C
Reflectivity	0.094–0.135 (0.112)	0.560–0.654 (0.596)	0.032–0.065 (0.043)
Emissivity	0.766–0.834 (0.807)	0.868–0.903 (0.886)	0.772–0.839 (0.811)
Material	Asphalt shingle	Green Roof	
Color	White		
Image			
Surface temperature	M1: 32.0 °C, M2: 31.7 °C	M1 (soil): 37.9 °C , M2 (vegetation): 29.8 °C , M3 (soil): 38.8 °C	
Reflectivity	0.510–0.622 (0.555)	0.074–0.142 (0.100)	
Emissivity	0.864–0.881 (0.875)	0.816–1.000 (0.898)	

3. Net Radiant Energy

The measured net radiant energy, which refers to the difference in the inflow of radiant energy and emitted radiant energy, was compared according to roof type. Herein, radiant energy refers to the summation of solar and terrestrial radiant energies. Thus, high net radiant energy means that emitted radiant energy is lower than that of inflow and that energy is accrued on the surface.

Figure 4 shows that white roofs, P-W and A-W, had significantly lower net radiant energy compared with other roof types. This result indicates that a smaller amount of energy was accumulated on the surface. Green roofs had the highest measured net radiant energy; it is likely that large amounts of energy were absorbed by the soil and vegetation.

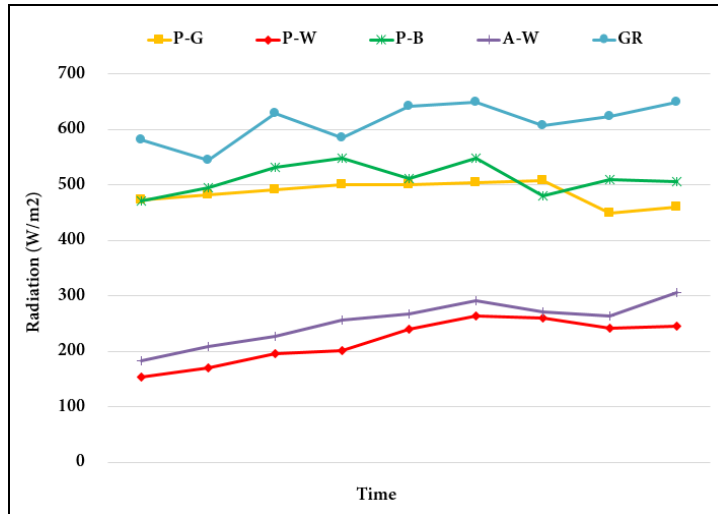
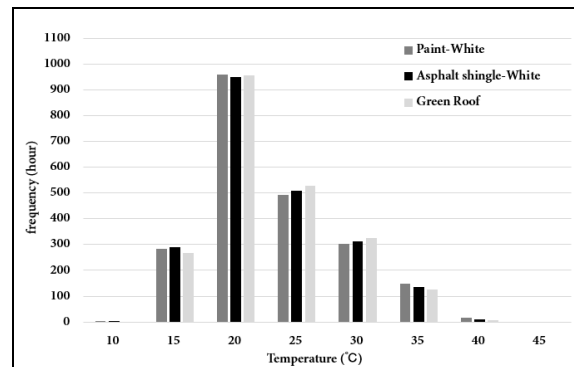
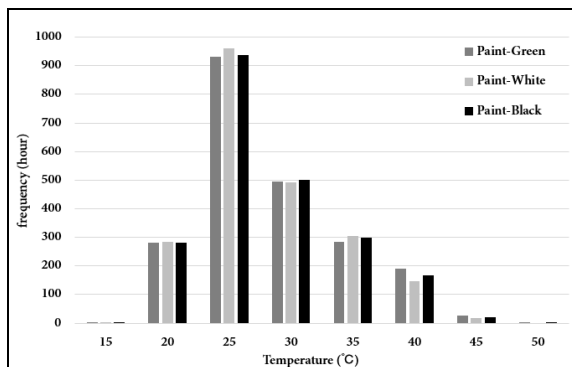


Fig 4. Changes in net radiant energy according to roof type.

4. Indoor temperatures

Summertime indoor temperatures are associated with air conditioning. That is, as indoor temperatures rise, greater amounts of energy will be used to lower the temperature. Thus, when indoor temperatures exceed those of air conditioning, energy consumption will increase.

The frequency of incidences in which indoor temperatures exceeded 26 °C, South Korea's standard air-conditioning temperature, was gathered to compare indoor temperatures. According to color, the frequency of such excessive indoor temperatures was 962, 994, and 991 h for white, green, and black roofs, respectively; white roofs showed the lowest frequency. This indicates that white roofs are more effective for lowering air-conditioning costs than those of green or black. Although the difference in the frequency of high indoor temperatures between white and green roofs was 32 h and may therefore appear small, it is actually significant because the aforementioned indoor temperatures actually range from 26 °C to 50 °C. Indoor temperatures were also compared according to roof materials. However, with 962 h of high indoor temperatures for paint and 968 h for asphalt shingles, no significant differences were observed. In the case of green roofs, the frequency of indoor temperatures exceeding 26 °C was 985 h, which is a significantly higher value than that of white roofs. This likely occurred because the heat accumulated in the soil could not be released at a sufficiently rapid pace and was thus accumulated.



Indoor temperature according to roof color.

Indoor temperature according to roof material.

Fig 5. Changes in indoor temperature according to roof type.

Conclusions

The current study investigated the use of cool roofs in mid-latitude temperate climate zones by using model buildings. By differing roof materials and colors, the present study investigated the types of roofs that could have UHI-mitigating effects.

The results showed that color had more influence than material on roof surface temperatures. Thus, even if the roof material is retained, low accumulation levels of radiant energy and low surface temperatures may be obtainable and can mitigate UHI effects, as long as the roof colors are brightened. Brighter roof colors may also allow indoor temperatures to be maintained at lower levels, thus lowering air-conditioning costs. Cool roofs may be effectively used on buildings and environments unsuited for green roofs.

Acknowledgment

This study was supported by the R&D program on environmental technology development implemented by the Gyeongnam Green Environment Center.

References

- [1] UN(United Nations). World Urbanization Prospects. The 2014 Revision Highlights. 7-12
- [2] Dewan, A. M., Yamaguchi, Y., 2009: Land use and land cover change in Greater Dhaka, Bangladesh: Using remote sensing to promote sustainable urbanization. *Applied Geography*, 29, 390-401
- [3] Jusuf, S. K., Wong, N.H., Hagen, E., Anggoro, R., Hong, Y., 2007: The influence of land use on the urban heat island in Singapore. *Habitat International*, 31, 232-242
- [4] Chen, X.L., Zhao, H. M., Li, P.X., Yin, Z. Y., 2006: Remote sensing image-based analysis of the relationship between urban heat island and land use/cover changes. *Remote Sensing of Environment*, 104, 133-146
- [5] Li, J. J., Wang, X. R., Wang, X. J., Ma, W. C., Zhang, H., 2009: Remote sensing evaluation of urban heat island and its spatial pattern of the Shanghai metropolitan area, China. *Ecological Complexity*, 6, 413-420
- [6] Synnefa, A., Dandou, A., Santamouris, M., Tombrou, M., Soulakellis, N., 2008: On the use of cool materials as a heat island mitigation strategy. *Journal of Applied Meteorology and Climatology*, 47, 2846–2856.
- [7] Akbari, H., Konopacki, S., 2005: Calculating energy-saving potentials of heat-island reduction strategies. *Energy Policy*, 33, 721–756.